Amino acid hydrogen oxalate quasiracemates – hydrocarbon side chains

Journal:	*CrystEngComm*
Manuscript ID	CE-ART-09-2021-001213.R2
Article Type:	Paper
Date Submitted by the Author:	01-Nov-2021
Complete List of Authors:	Wells, Russell; Whitworth University, Chemistry Sahlstrom, Katriel; Whitworth University, Chemistry Ekelem, Franklin; Whitworth University, Chemistry Wheeler, Kraig; Whitworth University, Chemistry

SCHOLARONE™
Manuscripts

ARTICLE

Amino acid hydrogen oxalate quasiracemates – hydrocarbon side chains

Russell G. Wells,[a] Katriel D. Sahlstrom,[a] Franklin I. Ekelem,[a] and Kraig A. Wheeler [a*]

Amino acid quasiracemates – generated from the assembly of pairs of chemically distinct amino acids of opposite handedness – continue to provide important opportunities to understand how self-assembly can be promoted despite using components with drastically different sizes and molecular shapes. Previous studies by Görbitz *et al.* and others cataloged 32 crystal structures of amino acid quasiracemates, with each showing the building blocks aligned with near inversion symmetry similar to their racemic counterparts. This investigation examined the impact of using a secondary coformer molecule, hydrogen oxalate, on the cocrystalline landscape of amino acid quasiracemates with hydrocarbon side chains. Eight racemic (4) and quasiracemic (4) hydrogen oxalate structures were generated. Crystal structures of these systems show the hydrogen oxalate moieties assembled into $C(5)$ molecular columns by the construction of robust O-H···O$^-$ hydrogen bonds with the amino acid enantiomers and quasienantiomers linked to these column motifs using a complex blend of N$^+$-H···O$^-$, O-H···O$^-$, and N$^+$-H···O=C contacts. The racemates and quasiracemate form similar packing motifs; however, due to the chemically non-identical nature of the quasiracemic components, the outcome is that the amino acids organize with near inversion symmetry. Both the conformational similarity (χ_{RMS}) and degree of inversion symemtry (C_i) of related pairs of quasienantiomeric components have been systematically assessed using readily available structural tools. This study shows how coformer molecules such as hydrogen oxalate can provide new and critical insight into the molecular recognition process of quasiracemic materials.

Introduction

For several years we have been interested in the class of compounds known as quasiracemates or quasiracemic materials[1,2] to probe the role of molecular shape in supramolecular assembly. These materials result from the pairwise alignment of near enantiomers and have proven useful for examining such areas as molecular recognition profiles[3-5], asymmetric transformations[6,7], and chemical separations[8,9]. The majority of our previous reports on quasiracemic systems followed a design strategy that included neutral small organic molecules that often limited the use of hydrogen bond contacts and other strong cohesive forces.[10-14] These investigations effectively showed that molecular shape can play a principal role in the construction of molecular assemblies. Our recent focus turned to understand how increased crystal lattice stabilization impacts the structural boundary of quasiracemate formation. One such investigation achieved 27% greater crystal stability by systematically increasing the size of a diarylamide molecular framework by replacing a pendant phenyl group with

a naphthyl substituent.[10] An indication of the importance of this structural change comes from the successful pairing of H·NO$_2$ substituents quasienantiomers. For the larger naphthylamide molecular scaffold, a crystal structure of the material was produced, while in the case of the smaller diarylamide[11], pairing the H·NO$_2$ quasienantiomeric components lacked any indication of molecular assembly from solution or the melt. Studies presented in this article continue our efforts to examine the role of increased lattice stabilization to quasiracemate formation by exploiting the use of strong directional hydrogen bonds present in amino acid quasiracemic structures and the robust motifs generated by use of hydrogen oxalate (HOx) anions.
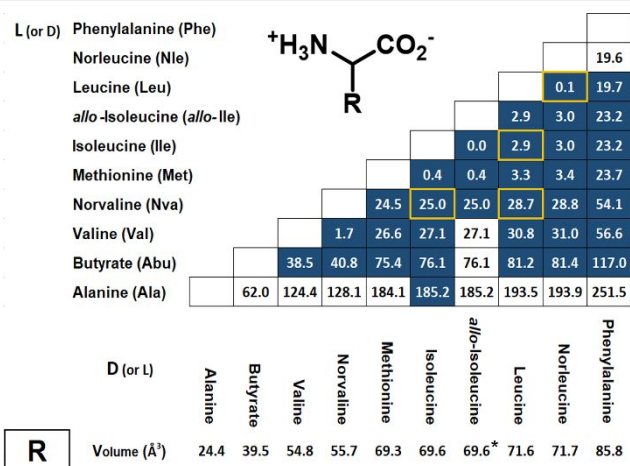
a. Department of Chemistry, Whitworth University, 300 West Hawthorne Road, Spokane, Washington, 99251, USA. E-mail: kraigwheeler@whitworth.edu.

ARTICLE   Journal Name

The selection of amino acid components for this study follows a logical approach to quasiracemate synthesis by offering easy access to chiral materials with increased crystal lattice stabilization. Because amino acids often exist in the zwitterionic form, they routinely promote strong crystal packing networks *via* charge-assisted hydrogen bonds.[15] The second benefit amino acids provide relates to the scope of available structural information of quasiracemic materials. The rich history of amino acid quasiracemates dates to the late 1990's when Görbitz and coworkers showed that simple cocrystallization studies using pairs of chemically distinct L and D amino acids resulted in crystal structures closely resembling the strict centrosymmetric alignment found in their racemic counterparts.[16-20] As shown in Fig. 1, this early structural study (25 entries) and those from recent efforts (7 entries)[20-25] contribute to the 32 known amino acid quasiracemic crystal structures. It should also be noted that attempts to cocrystallize other quasiracemic systems resulted in only unit cell parameters from poor quality crystals (L-*allo*-isoleucine (*allo*-Ile)·D-norvaline (Nva) and L-*allo*-Ile·D-methionine (Met) systems, ref. 26) or spontaneous resolution (*allo*-Ile·alanine (Ala), *allo*-Ile·butyrate (Abu), *allo*-Ile·valine (Val), and Ala·leucine (Leu), ref. 15). While the success from several of these systems might be largely anticipated due to the structural similarity of the amino acid pair [Abu·Nva, Met·norleucine (Nle) and leucine·isoleucine (Ile)] other outcomes emerge from this set as more remarkable given the considerable difference in molecular shapes and sizes of the components [Ala·Ile, Val·Nle and Abu·phenylalanine (Phe)]. The significance of these findings can be gauged by considering the extant database of neutral small molecule quasiracemates where a common structural theme is pairing H·F[11] and Cl·Br[12,13,27-29] quasienantiomers to generate quasiracemates. In contrast to these relatively small topological differences, the set of amino acid quasiracemates shown in Fig. 1 provides greater structural variance of the quasienantiomeric components. This difference in structural framework starts with the H·CH₃ pair as seen with the Abu·Val, Abu·Nva, Val·Ile, Nva·Ile, Nva·Leu, and Nva·Nle systems and extends to the CH₃·C₆H₅ substitution pattern of Abu·Phe.
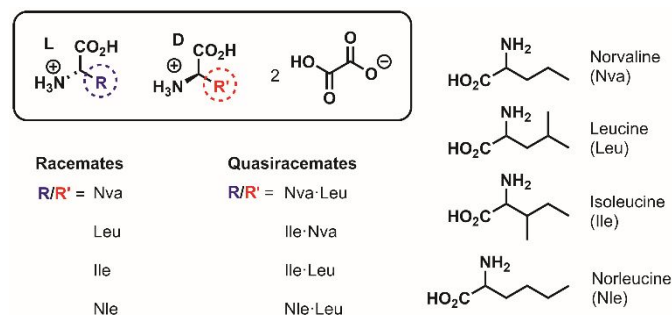

Fig. 2 Racemic and quasiracemic amino acid hydrogen oxalate systems examined in the current study.

The current investigation re-examines the structural space of four of these amino acid quasiracemic systems – *i.e.,* Nva·Ile, Nva·Leu, Leu·Ile, and Leu·Nle - by introducing oxalic acid as a secondary coformer molecule (Fig. 2). Outcomes from these new systems are compared in light of several related racemic hydrogen oxalates and previously reported bimolecular amino acid quasiracemates with a focus on the topological similarity of the amino acid components. An understanding of these structural similarities is achieved by assessing how well the structures approximate inversion symmetry and the degree of conformational similarity of the quasienantiomers. This report emphasizes amino acid components with hydrocarbon side chains and a subsequent article in this journal targets the structural impact of sulfur-containing amino acids. Together, these reports show how the addition of a secondary coformer molecule such as hydrogen oxalate to quasiracemate formation creates complex and robust crystal structure motifs capable of creating decidedly non-centrosymmetric assemblies not previously observed in quasiracemic crystal structures.

Results and discussion

Racemic and quasiracemic amino acid hydrogen oxalates

The eight racemic (4) and quasiracemic (4) amino acid-hydrogen oxalate systems examined in this report were prepared by slow evaporation of aqueous solutions consisting of a 2:1:1 ratio of the oxalic acid, L-amino acid, and D-amino acid components. Each generated X-ray crystal structure shows the components in the amino acid⁺-H hydrogen oxalate form, where the proton associated with one of the oxalic acid carboxyl groups is transferred to the amino acid carboxylate (Table S1†, Fig. 3). The significance of this acid-base process is that it creates cocrystalline molecular salts where the set of hydrogen-bond donor groups participates in an extensive network of nonbonded contacts. Figure 3A shows the packing diagrams of a model system – *i.e.,* DL-leucinium hydrogen oxalate (space group $P\bar{1}$) (previously reported in the CCDC *Cambridge Structural Database*[30] as refcode WIPQOE[31]) - and the various structural features shared with the other racemic and quasiracemic structures. Charge-assisted hydrogen bonds

dominate this structure and occur *via* hydrogen oxalate-hydrogen oxalate (O-H···O⁻), hydrogen oxalate-leucinium (2 N⁺$_{leucinium}$-H···⁻O₂C$_{HOx}$ and O$_{leucinium}$-H···⁻O₂C$_{HOx}$), and leucinium-leucinium (N⁺-H···O=C) interactions. These molecular assemblies form rigorously centrosymmetric L-leucinium···D-leucinium assemblies with $R_2^2(10)$ graph-set notation[32,33], while the hydrogen oxalate components align into translationally related *C*(5) chains. When viewed together, the leucinium and hydrogen oxalate molecules further assemble to give $R_4^4(15)$ motifs (Fig. 3B).
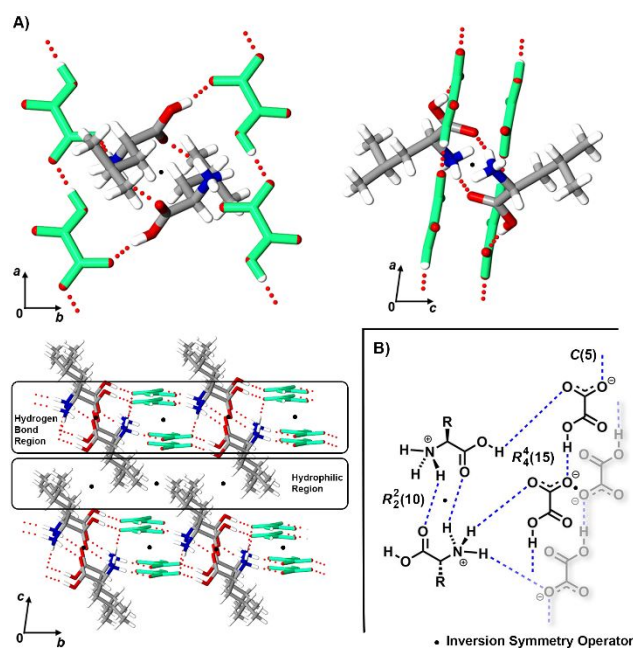

Fig. 3 The structure of DL-leucinium hydrogen oxalate showing A) three views of crystal structure packing and B) a diagram depicting common hydrogen-bond motifs.

Close inspection of these crystal structures reveals that the hydrogen oxalate coformer molecules participate in dominant packing motifs that provide a common structural theme for all amino acid-hydrogen oxalate systems. In the case of the racemic leucinium hydrogen oxalate system (Fig. 3A), the *C*(5) motifs occur *via* strong O-H···O⁻ interactions where the O···O⁻ distance is 2.613(1) Å with a nearly linear ∠O-H···O⁻ angle (175(2)°). This chain motif aligns with a neighboring inversion related hydrogen oxalate chain to create molecular columns with a short stack distance of 3.04 Å. The next closest set of hydrogen oxalate columns are translationally related with spacing corresponding to the *b* axis (9.56 Å). These hydrogen oxalate columns provide a consistent scaffold in the crystal where the leucinium components link *via* N⁺$_{leucinium}$-H···⁻O₂C(hydrogen oxalate) and O$_{leucinium}$-H···⁻O₂C(hydrogen oxalate). Another identifying feature of the DL-Leu·HOx structure relates to crystal organization, where the hydrophilic (CO₂⁻, NH₃⁺ and HOx anions) and hydrophobic (*R* groups) structural features align into distinct crystal regions that alternate in the ab plane. This bilayer pattern in the crystal creates a 2D array of dominant non-bonded contacts that involve the amino acid cations and

hydrogen oxalate anions with the tail ends of the amino acids assembling using van der Waals surfaces.

With the exception of DL-Ile·HOx (*P*2₁/*n*), each racemic [*P*$\bar{1}$; DL-Nva·HOx and DL-Nle·HOx (Fig. S1)] and quasiracemic [*P*1; L-Nva·D-Leu·2HOx, L-Ile·D-Nva·2HOx, L-Ile·D-Leu·2HOx, and L-Nle·D-Leu·2HOx] hydrogen oxalate structure provided in this study exhibit a high degree of isostructurality with similar datasets and unit cell parameters to the DL-Leu·HOx example. In these cases – including DL-Ile·HOx – this collection of amino acid hydrogen oxalates form nearly identical crystal packing patterns. As such, these structures also assemble using a similar set of contacts (N⁺-H···O⁻, O-H···O⁻, and N⁺-H···O=C) that create a network of hydrogen bonds described by a common set of graph-set descriptors (Fig. 3B). The structures show pairs of D and L amino acids bordered by hydrogen oxalate columns ranging from 9.49 to 9.86 Å depending on the steric features of the amino acid side groups (*R*). For the quasiracemic systems, the pairs of amino acid quasienantiomers and hydrogen oxalate columns organize into motifs that mimic the packing patterns observed in the racemic structures. While very similar, the molecular alignment in these cases is strictly noncentrosymmetric due to use of chemically unique quasienantiomeric components.

In general, the crystals and amino acid components in the crystal structures were well behaved. DL-Nle·HOx provides the exception to this trend where the crystals grow as curved needles with the Nle fragments exhibiting whole-molecule disorder. This suggests that the bilayer crystal landscape of DL-Nle·HOx supports multiple Nle orientations likely due to the weak interactions at the interface of the amino acid side chains (Fig. S1).
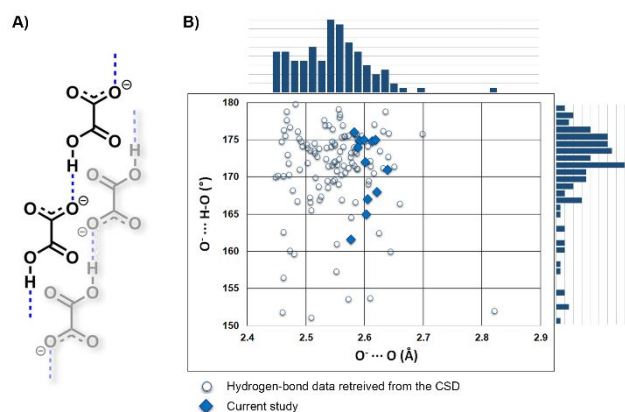

Fig. 4 A) Stacking motif of neighboring hydrogen oxalate chains and B) a scatterplot of O···O⁻ and ∠O-H···O⁻ hydrogen-bond parameters.

Hydrogen oxalate coformer structural tendencies

We wondered if the hydrogen-bonded motifs and close stacking of the hydrogen oxalate chains observed in the current set of crystal structures transfers to other known systems. A search of the *CCDC-Cambridge Structural Database*[30] (CSD, version 5.42, update 2) for O-H···O⁻ hydrogen oxalate-hydrogen oxalate

interactions revealed 120 contacts from 99 CSD entries with average $O\cdots O^-$ distances and $\angle O\text{-}H\cdots O^-$ angles of 2.55 Å and 170.9°, respectively (Fig. 4). In such cases, these hydrogen oxalate interactions generate molecular chains where the components are either translation (85), glide (21), or screw (14) symmetry related. These structures occur by pairing hydrogen oxalate with a variety of molecular and atomic cations such as quaternary amine (68), amino acid (14), pyridinium (9), atomic cationic (4), and triazolium (2) components. 18 of these entries exist with multiple molecules in the asymmetric unit ($Z' > 1$). Of the 99 CSD entries, over half (50) of the structures exhibit close stacking of the hydrogen oxalate chains with 31 entries forming pairs of stacked chains similar to the leucinium hydrogen oxalate example shown in Fig. 3A and 19 of these structures forming infinite stacks of hydrogen oxalate chains. This CSD search shows the structural breadth of hydrogen oxalate as a coformer participant with a variety of molecular and atomic cations. Perhaps the most striking structural feature of the oxalate moiety is its ability to form persistent supramolecular chain/stacking architectures that further serve to align the principal amino acid components *via* strong donor-H$\cdots$O$^-$ contacts. The 8 systems included in this study generate 12 unique $O\text{-}H\cdots O^-$ hydrogen oxalate-hydrogen oxalate interactions with hydrogen bond parameters that closely compare to the CSD study with an average $O\cdots O^-$ distance of 2.60 Å and a $\angle O\text{-}H\cdots O^-$ angle of 171.2°. These hydrogen oxalate motifs provide considerable crystal lattice stabilization that permits the pairing of structurally diverse amino acid components.

Quasiracemates – *R* group volumes, molecular conformations, and near inversion symmetry

Looking beyond the supramolecular motifs described in this study, we turn our attention to several methods that provide useful insight to the molecular topology and crystal packing differences of amino acid quasienantiomeric components. These methods target the variation in group volumes, spatial arrangement of the side groups, and the near symmetry alignment of the quasienantiomeric components.

Recently, we approximated the topological difference between pairs of quasienantiomers by tabulating the percent difference in volume (%ΔV) of functional groups for a family of naphthylamides.[10] While not a true indicator of molecular shape, this approach has proven useful as a diagnostic tool to assess the variation of shape space for sets of molecular fragments. For example, the H·F and Cl·Br substitution patterns commonly used in quasiracemic design strategies give %ΔV values of 60 and 16, respectively. By comparison, one of the smallest imposed structural difference associated with assembling amino acid quasienantiomers is the H·CH$_3$ pair where %ΔV = 100% (‡). This information, and that provided in Fig. 1, suggests the amino acid framework offers an important

entry point to explore molecular recognition events using components with greater structural diversity.

Fig. 1 provides %ΔV data for each pair of amino acid side groups (*R*). These estimated *R* group volumes were determined by removing $^-O_2C\text{–}CH\text{-}NH_3^+$ component from the reported partial molar volume of amino acids (**§**).[34] This %ΔV data correlates with the expected variation in pendant alkyl group sizes and this difference is most prominent with straight chain systems such as in the case of pairing alanine with amino acids of increasing chain length [Ala·Abu (%ΔV = 62.0), Ala·Nva (%ΔV = 128.1), and Ala·Nle (%ΔV = 193.9)]. When this method is applied to the 32 cocrystallization successes, the %ΔV information offers an effective quantitative measure of the scope of these successes (Fig. 1). While some of the entries may have been anticipated due to the structural similarity of the components [Met·Nle (%ΔV = 3.4) and Leu·Ile (%ΔV = 2.9)], other successful entries combine amino acids with significantly different *R* groups [Abu·Phe (%ΔV = 117.0) and Ala·Ile (%ΔV = 185.2)]. In addition to providing a quantitative gauge of the existing quasiracemic systems, another benefit of this method is that it can be used as a predictive tool. Of the 45 entries provided in Fig. 1, eleven of the crystal structures remain unreported and relate to the alanine, *allo*-isoleucine, and phenylalanine systems. Does the absence of these entries relate to attempts to pair ill-suited quasienantiomers or are these omissions simply an artefact of uncharted territory where the cocrystallization experiments have yet to be fully examined? The answer is likely yes to both questions. Inspection of the %ΔV data in Fig. 1 indicates Ala·Ile (%ΔV = 185.2) as the system reported with the largest percent volume difference of the component *R* groups. Though the Ala·Ile entry is quite significant, it is possible that other systems near or exceeding this %ΔV threshold lack the necessary structural complementarity of the quasienantiomeric components for cocrystal formation. Equally important to point out are the four systems with %ΔV values < 100 (Ala·Abu, *allo*-Ile· Abu, *allo*-Ile· Val, and Nle·Phe). The absence of these entries may reflect the lack of focused attention to these quasienantiomeric pairs rather than unsuccessful cocrystallization attempts. As such, this %ΔV information suggests that cocrystallization of these amino acid quasienantiomers could result in the expected quasiracemates.
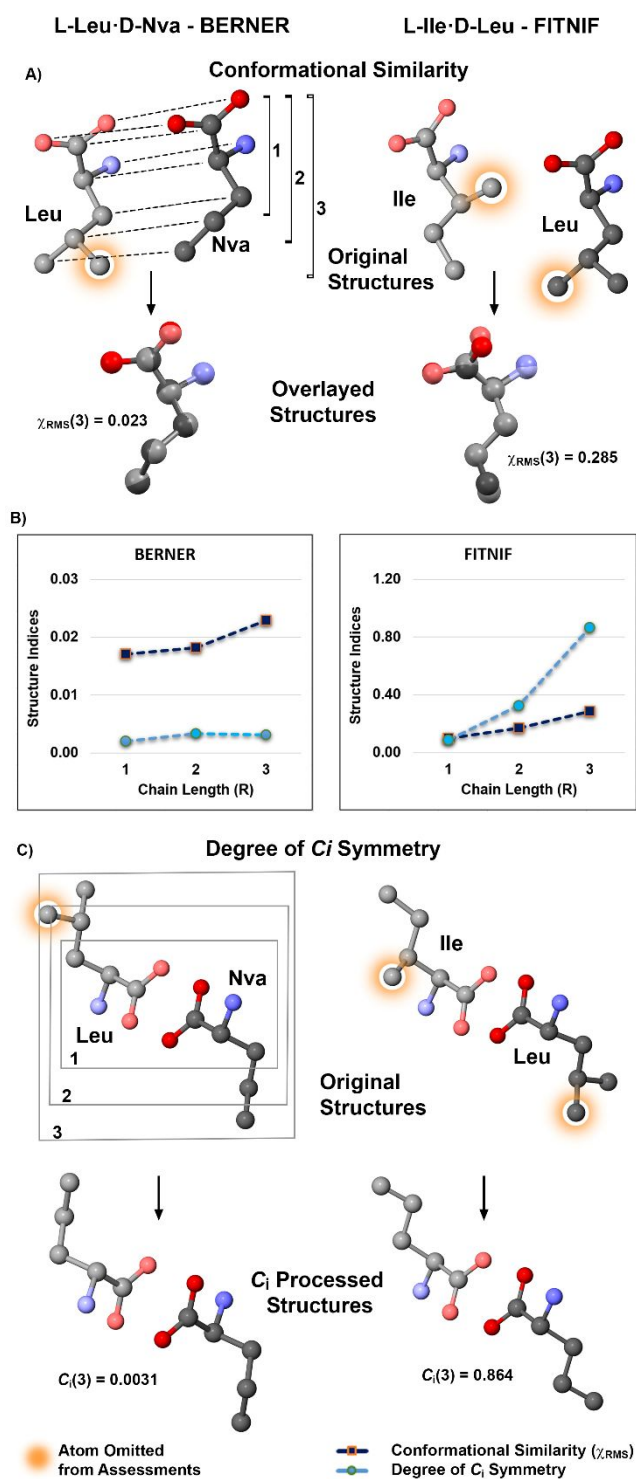
Fig. 5 Crystal structures of L-leucine·D-norvaline (BERNER) and L-isoleucine·D-leucine (FITNIF) showing the A) strategy for conformational overlays, B) plots of tabulated structure indices χ_{RMS} and C_i data and C) degree of inversion symmetry (C_i). Original D amino acid isomers indicated by dark grey carbon atoms.

The next two methods assess the conformational similarity (χ_{RMS}) and degree of inversion (C_i) symmetry that relates pairs of quasienantiomeric components. As shown in Fig. 5, the Leu·Nva (CSD reference code BERNER) and Leu·Ile (FITNIF) structures offer model systems to describe these techniques.

The structure overlay feature provided in the *CCDC-Mercury* program[35] was used to process the conformational similarities of each quasienantiomeric pair. This process involved inverting the chirality of one component, omitting the hydrogen atoms, and then selecting the appropriate pairs of atoms to process (Fig. 5A). Atoms without a corresponding partner were not included in the assessment – *i.e.,* for BERNER one atom was removed and for FITNIF two atoms were omitted from the calculations (Fig 5A, orange highlights). The root-mean-square (χ_{RMS}) calculation determines the degree of overlay with χ_{RMS} values near zero indicting a close match of the molecular fragments. The flexibility in atom selection is an important feature of the *CCDC-Mercury* resource. When this approach is applied to the amino acid quasiracemate structures, the degree of structural overlay can be measured as a function of *R* group chain length (Fig. 5B). In each case, the core O_2C-C(C)-N fragment is nearly conformationally identical with the attached *R* group chain providing the point of structural divergence. For BERNER, the CCDC-*Mercury* overlay calculations gave an insignificant increase in χ_{RMS} values with increasing chain length (0.02, 0.02, 0.02) as compared to those tabulated for FITNIF (0.10, 0.17, 0.29).

Avnir and coworkers have developed the *Continuous Symmetry Measures* method that quantitatively evaluates the degree of basic symmetries present in structural motifs.[36-38] The measured value obtained ranges from zero (the motif has the investigated symmetry) to an upper limit of 100. By processing data in a similar manner to the *CCDC-Mercury* overlay approach, we were able to determine the extent of inversion symmetry (C_i) these model structures exhibit as a function of chain length (Fig. 5C). The C_i data generated for both BERNER and FITNIF are quite revealing. The Nva·Leu quasienantiomers in BERNER align in the crystal with nearly idealized inversion symmetry (C_i = 0.002, 0.003, 0.003) while the Ile·Leu components for FITNIF are decidedly less centrosymmetric (C_i = 0.09, 0.33, 0.86) (Fig. 5B). The combined use of the conformational similarity (*CCDC-Mercury structure overlay*) and degree of symmetry (C_i) approaches offers an important strategy for understanding the organization of quasiracemic structures. For the BERNER structure, the two quasienantiomeric components possess similar molecular conformations that effectively align with near inversion symmetry. In the case of FITNIF; however, the Ile·Leu components take on similar molecular shapes, but these molecules assemble into motifs that deviate to a greater extent from C_i symmetry.
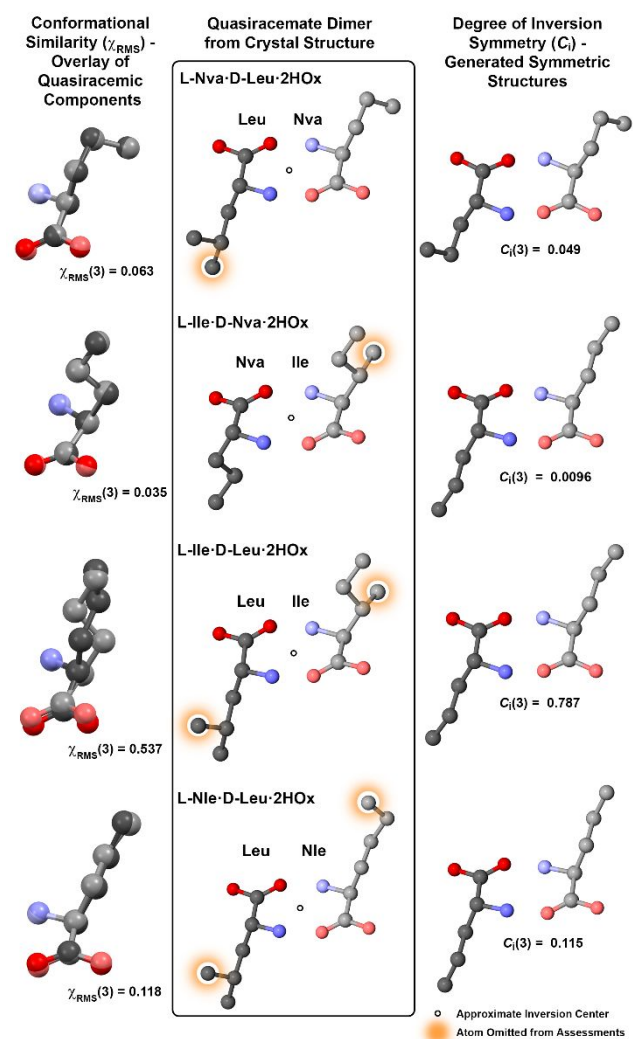
ARTICLE

Fig. 6 Crystallographic data showing amino acid quasiracemic dimers and graphical output from conformational similarity (χ_{RMS}) and degree of inversion symmetry (C_i) assessments. Original D amino acid isomers indicated by dark grey carbon atoms.
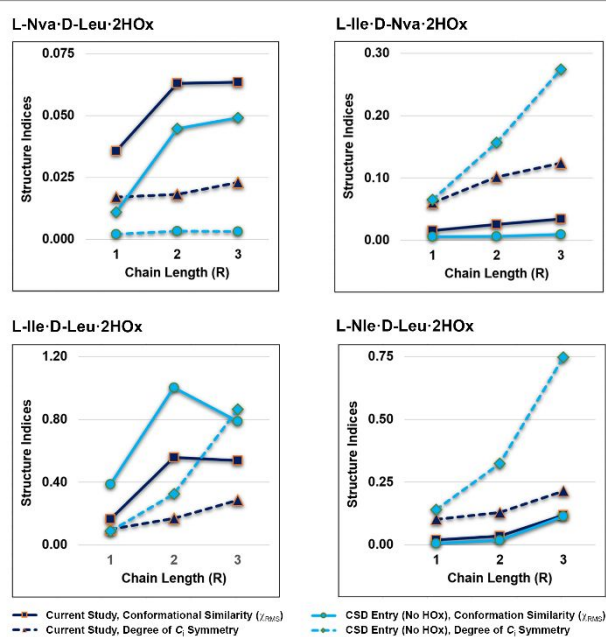

Fig. 7 C_i and χ_{RMS} structure indices for the amino acid hydrogen oxalate quasiracemates.

The application of the *CCDC-Mercury* overlay (χ_{RMS}) and C_i symmetry methods to the current set of amino acid hydrogen oxalate quasiracemates offers a unique opportunity to assess the spatial variance of quasienantiomeric components in these systems. Similar to the BERNER and FITNIF examples (Fig. 5), the calculations for these crystal structures were systematically processed by varying the chain length of the amino acid pair (Fig. 6). The hydrogen oxalate molecules were omitted from these calculations because their column motifs closely match centrosymmetric alignment. Outcomes from this study were compared to the non-hydrogen oxalate quasiracemate structures found in the literature. Fig. 7 provides the degree of inversion symmetry (C_i) and conformational similarity (χ_{RMS}) for pairs of amino acid components. For the Ile·Nva·2HOx and Nva·Leu·2HOx systems, the low χ_{RMS} values indicate similar molecular shapes for the amino acid components. Comparatively, these structures are more effective at inversion alignment of the components since the C_i values are less than 0.1. The other two systems – Ile·Leu·2HOx and Nle·Leu·2HOx – align molecules in the crystal with higher χ_{RMS} and C_i values demonstrating a greater variation in molecular conformations and inversion symmetry.

The C_i and RMS information summarized in Fig. 8 corresponds to calculations utilizing the entire amino acid molecule. This information shows that while the use of hydrogen oxalate as a coformer molecule promotes the formation of three-component amino acid quasiracemic systems, the alignment of the components in these systems does not differ drastically from the non-HOx literature examples. In fact, three of the four non-HOx structures exhibit larger χ_{RMS} and C_i values than the hydrogen oxalate counterparts.
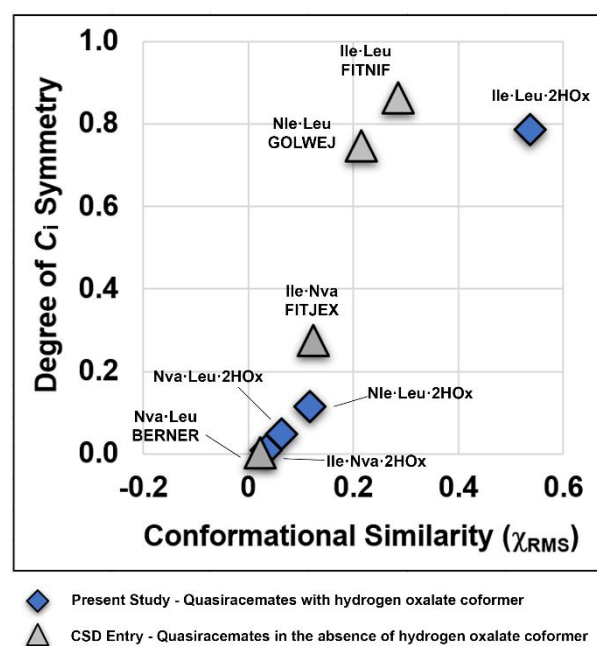

Fig. 8 Assessment of the conformational similarity (χ_{RMS}) and degree of inversion (C_i)

symmetry for pairs of quasienantiomeric components for entries from the present study and CSD. Values correspond to $\chi_{RMS}(3)$ and $C_i(3)$.

Conclusions

The outcomes from this study underscore the role of increased crystal lattice stabilization to the success of quasiracemate formation. Amino acids offer an interesting addition to quasiracemic materials because they provide easy access to structurally diverse quasienantiomeric components assembled from extensive networks of charge-assisted non-bonded contacts. This study produced three new racemates and four new crystalline phases of known amino acid quasiracemates by the addition of a secondary hydrogen oxalate coformer molecule. The crystal structures of these systems show the hydrogen oxalate moieties assembled into $C(5)$ molecular columns by construction of robust O-H···O⁻ hydrogen bonds. The amino acid enantiomers and quasienantiomers are then linked to these column motifs using a complex set of N⁺-H···O⁻, O-H···O⁻, and N⁺-H···O=C contacts. While the racemates and quasiracemate form similar packing motifs, because the quasiracemates are constructed from chemically non-identical components, the outcome is that the amino acids organize into near inversion symmetry.

Several structural tools were applied to these multi-component systems to understand the spatial diversity of the amino acid building blocks. Since the majority of quasiracemates organize into assemblies that mimic the inversion relationships observed in racemates, we were interested in examining the level of symmetry-distortion that the pair of amino acid components exhibit. Crystal structures generated from this study and those retrieved as non-hydrogen oxalate forms from the *CCDC-CSD* were assessed. Avnir's *Continuous Symmetry Measures* and the structure overlay feature in *CCDC-Mercur*y were used to evaluate the degree of inversion symmetry and conformational similarity of the components. Use of these structural tools showed that one structure (Ile·Leu·2HOx) achieved a conformational similarity index (χ_{RMS}) greater than 0.5 and four structures (Ile·Leu·2HOx, FITNIF, GOLWEJ, FITJEX) possess packing motifs distorted from inversion symmetry with C_i values greater than 0.2. The use of these methods with quasiracemic materials offers important advances in understanding the factors responsible for the assembly of quasienantiomers.

Author Contributions

Investigation, formal analysis, and visualization (RGW, KDS, FIE, and KAW). Conceptualization, methodology, supervision, and writing - original draft (KAW).

Conflicts of interest

There are no conflicts to declare.

Acknowledgements

Notes and references

‡ %ΔV = |V1-V2|/[(V1+V2)/2]

§ Amino acid R group volumes were determined by subtracting the volume of the -O₂C-CH-NH₃⁺ fragment (V_{O2C-CH-NH3} = V_{glycine} (43.24 Å3) − V_H (7.2 Å³, ref. 10) from V_{amino acid} supplied in ref. 32.

1   A. Fredga, *Bull. Soc. Chim. Fr.*, 1973, **1**, 173 – 182.
2   Q. Zhang and D. P. Curran, *Chem. – Eur. J.*, 2005, **11**, 4866 – 4880.
3   M. M. H. Smets, E. Kalkman, A. Krieger, P. Tinnemans, H. Meekes, E. Vlieg and H. M. Cuppen, IUCrJ, 2020, **7**, 331 – 341.
4   S. B. H. Kent, *Cur. Opin. Chem. Biol.*, 2018, **46**, 1 – 9.
5   T. Hasell, M. A. Little, S. Y. Chong, M. Schmidtmann, M. E. Briggs, V. Santolini, K. E. Jelfs and A. I. Cooper, *Nanoscale*, 2017, **9**, 6783 – 6790.
6   U. K. Shrestha, A. E. Golliher, T. D. Newar, F. O. Holguin and W. A. Maio, *J. Org. Chem.*, 2021, **86**, 11086 – 11099.
7   Y. Lu, A. J. Bolokowicz, S. A. Reeb, J. D. Wiseman and K. A. Wheeler, *RSC Adv.*, **4**, 8125 – 8131.
8   M. H. Bosits, E. Pálovics, J. Madarász and E. Fogassy, *J. Chem.*, 2019, 4980792.
9   S. Mane, *Anal. Methods*, 2016, **8**, 7567 – 7586.
10   D. E. Craddock, M. J. Parks, L. A. Taylor, B. L. Wagner, M. Ruf and K. A. Wheeler, *CrystEngComm*, 2021, **23**, 210 – 215.
11   I. C. Tinsley, J. M. Spaniol and K. A. Wheeler, *Chem. Commun.*, 2017, **53**, 4601 – 4604.
12   J. T. Cross, N. A. Rossi, M. F. Serafin and K. A. Wheeler, *CrystEngComm*, 2014, **16**, 7251 – 7258.
13   M. Hendi, P. Hooter, V. Lynch, R. E. Davis and K. A. Wheeler, *Cryst. Growth Des.*, 2004, **4**, 95 – 101.
14   S. Fomulu, M. Hendi, R. E. Davis and K. A. Wheeler, *Cryst. Growth Des.*, 2002, **2**, 645 – 651.
15   C. H. Görbitz, *Crystallogr. Rev.*, 2015, **21**, 160 – 212.
16   C. H. Görbitz, K. Rissanen, A. Valkonen and A. Husabø, *Acta Crystallogr., Sect. C: Cryst. Struct. Commun.*, 2009, **C65**, o267 – o272. L-Phe·D-Abu (CSD ref. code: POVYEF), L-Phe·D-Nva (POVYIJ), L-Phe·D-Met (POVYOP), L-Phe·D-Leu (POVYUV), L-Phe·D-Ile (POVZAC), L-Phe·D-*allo*-Ile (POXGAL).
17   B. Dalhus and C. H. Görbitz, *Acta Crystallogr., Sect. C: Cryst. Struct. Commun.*, 1999, **C55**, 1105 – 1112. D-Nle·L-Nva (GOLVIM), D-Nle·L-Met (GOLVOS), D-Nle·L-Val (GOLVUY), D-Nle·L-*allo*-Ile (GOLWAF), D-Nle·L-Leu (GOLWEJ).
18   B. Dalhus and C. H. Görbitz, *Acta Crystallogr., Sect. C: Cryst. Struct. Commun.*, 1999, **C55**, 1547 – 1555. L-Val·D-Abu (BERQAQ), L-Val·D-Nva (BERQEU), L-Val·D-Met (BERQIY), L-Leu·D-Abu (BERNAN), L-Leu·D-Nva (BERNER), L-Leu·D-Met (BERNIV), L-Leu·D-Val (BERPET).
19   B. Dalhus and C. H. Görbitz, *Acta Crystallogr. Sect. B Struct. Sci.*, 1999, **B55**, 424 – 431. L-Ile·D-Ala (FITHIZ), L-Ile·D-Abu (FITJAT), L-Ile·D-Nva (FITJEX), L-Ile·D-Nle (FITLEZ), L-Ile·D-Met (FITLID), L-Ile·D-Val (FITMEA), L-Ile·D-Leu (FITNIF).
20   M. M. H. Smets, E. Kalkman, P. Tinnemans, A. M. Krieger, H. Meeks and H. M. Cuppen, *CrystEngComm*, 2017, **19**, 5604 – 5610. D-Abu·L-Nva (VEDZUC, VEDZUC01).
21   C. H. Görbitz, D. S. Wragg, I. M. B. Bakke, C. Fleischer, G. Grønnevik, M. Mykland, Y. Park, K. W. Trovik, H. Serigstad and B. E. V. Sundsli, *Acta Crystallogr., Sect. C: Cryst. Struct. Commun.*, 2016, **C72**, 536 – 543. L-Abu·D-Met (ANUPOQ, ANUPOQ01 polymorphs).
22   C. H. Görbitz and P. Karen, *J. Phys. Chem. B*, 2015, **119**, 4975 – 4984. L-Nle·D-Met (VUQNAY).
23   C. H. Görbitz, B. Dalhus and G. M. Day, *Phys. Chem. Chem.*

Phys., 2010, **12**, 8466 – 8477. L-Abu·D-Nle (URODOV), L-*allo*-Ile·D-Leu (URODEL), L-Nva·D-Met (URODIP).

24 G. S. Prasad and M. Vijayan, *Acta Crystallogr., Sect. C: Cryst. Struct. Commun.,* 1991, **C47**, 2603 – 2606. L-Phe·D-Val (SONCED).

25 B. Dalhus and C. H. Görbitz, Acta Crystallogr. Sect. B Struct. Sci., 2000, **B56**, 720 – 727. L-Ile·D-*allo*-Ile (XADVED).

26 Dalhus B. Crystal structures of hydrophobic amino acid complexes – a multivariate analysis of hydrogen bond geometries. Ph.D. Dissertation. University of Oslo. Oslo, Norway, 2000. (L-*allo*-Ile·D-Nva, L-*allo*-Ile·D-Met)

27 J. M. Spaniol and K. A. Wheeler, *RSC Advances*, 2016, **6**, 64921 – 64929.

28 A. M. Lineberry, E. T. Benjamin, R. E. Davis, W. S. Kassel and K. A. Wheeler, *Cryst. Growth Des.*, 2008, **8**, 612 – 619.

29 F. Toda, K. Tanaka, H. Miyamoto, H. Koshima, I. Miyahara and K. Hirotsu, *J. Chem. Soc., Perkin Trans. 2*, 1997, 1877 – 1886.

30 C. R. Groom, I. J. Bruno, M. P. Lightfoot and S. C. Ward, *Acta Crystallogr. Sect. B Struct. Sci.*, 2016, **B72**, 171 – 179.

31 K. Manoj, H. Takahashi, Y. Morita, R. G. Gonnade, S. Iwama, H. Tsue and R. Tamura, *Chirality*, 2015, **27**, 405 – 410.

32 J. Bernstein, R. E. Davis, L. Shimoni and N.-L. Chang, *Angew. Chem. Int. Ed.*, 1995, **34**, 1555 – 1573.

33 M. C. Etter, *Acct. Chem. Res.*, 1990, **23**, 120 – 126.

34 S. Sirimulla, M. Lerma, W. C. Herndon, *H. Chem. Inf. Model*, 2010, **50**, 194 – 204.

35 C. F. Macrae, I. Sovago, S. J. Cottrell, P. T. A. Galek, P. McCabe, E. Pidcock, M. Platings, G. P. Shields, J. S. Stevens, M. Towler and P. A. Wood, *J. Appl. Cryst.*, 2020, **53**, 226 – 235.

36 P. Alemany, D. Casanova, S. Alvarez, C. Dryzun and David Avnir, "Continuous Symmetry Measures: A New Tool in Quantum Chemistry" Reviews in Computational Chemistry, Volume 30, Abby L. Parrill and Kenneth B. Lipkowitz, Editors, Chapter 7, p. 289 – 352, Wiley, 2017.

37 M. Pinsky, C. Dryzun, D. Casanova, P. Alemany and D. Avnir, *J. Comput. Chem.*, 2008, **29**, 2712 – 2721.

38 H. Zabrodsky, S. Peleg and D. Avnir, *J. Am. Chem. Soc.*, 1992, **114**, 7843 – 7851.